ANALYSIS AND IMPLEMENTATION OF THE SEMI-LAGRANGIAN TECHNIQUE

J.R. Bates

Irish Meteorological Service, Dublin.

Summary: The properties of some multiply-upstream semi-Lagrangian schemes for integrating the advection equation are analysed. It is shown that the schemes, though explicit, are unconditionally stable for a constant wind field. The results of applying the schemes to a split-explicit multilevel model where the adjustment terms are integrated using a forward-backward treatment of the gravity wave terms and a trapezoidal implicit treatment of the Coriolis terms are described. An alternating direction implicit method for integrating the adjustment terms is also presented. This is applied in conjunction with a semi-Lagrangian treatment of advection in a one-level model and found to give stable integrations for long time steps.

1. INTRODUCTION

The requirement of computational efficiency continues to have a high priority in NWP modelling, despite the advances in available computer power. The split explicit and semi-implicit time integration techniques have led to considerable gains in efficiency, the former having had the greatest impact in limited area grid point models and the latter in global spectral models.

The present lecture is concerned with the semi-Lagrangian technique, which is in essence a grid point technique. It has so far been applied only to limited area models, but it is possible that it could be applied with advantage to global models.

The situation at present prevailing with operational grid point models is that the errors associated with the spatial discretization greatly exceed those associated with the time discretization (Robert, 1981). There is therefore much scope for the development of efficient time schemes based on the use of longer time steps.

The semi-Lagrangian technique allows one efficiently to circumvent the limitation on the time step imposed by the CFL condition for advection. The essential step in achieving this, first introduced by Robert (1981), is to use multiply-upstream interpolation, whereby values of the variables at the departure points of particles are estimated by interpolating from gridpoints surrounding the departure points. Previous semi-Lagrangian models had estimated the values at departure points by interpolating from gridpoints surrounding the arrival points of the particles. Such models were subject to a CFL stability criterion for advection and gave no

material advantage over corresponding Eulerian models.

A semi-Lagrangian treatment of advection can be combined with various methods of treating the adjustment terms in the equations of motion. Robert (1981) applied the semi-Lagrangian technique only to the advection of vorticity and combined this with a semi-implicit treatment of the gravity wave terms in the divergence and continuity equations of a shallow water model. The latter two equations were treated in an entirely Eulerian manner. In a more recent paper, Robert (1982) has expressed the shallow water equations in momentum form and applied the semi-Lagrangian technique to all three material derivatives. The adjustment terms are treated in a semi-implicit manner. This has led to even greater stability when the model is run with long time steps than was found with the original method. No explicit comparison of the efficiency of the two methods has been given, however.

An analysis of the semi-Lagrangian technique applied to the advection equation, showing how the properties of the scheme depend on the method of interpolation, has been given by Bates and McDonald (1982). A further analysis has been given by McDonald (1983).

Bates and McDonald (1982) made the first application of the multiply-upstream semi-Lagrangian technique to a multi-level model. They applied the technique to the HIBU model, developed by F. Mesinger and Z. Janjic. This is a split explicit model which in its original Eulerian form combined an energy and enstrophy conserving treatment of advection with a forward-backward treatment of the pressure gradient terms and a trapezoidal implicit treatment of the Coriolis terms. When the semi-Lagrangian method was used to integrate the advective terms, treating the adjustment terms as before, it was found that a considerable gain in efficiency could be achieved. The split semi-Lagrangian treatment of advection combined with a forward-backward treatment of the pressure gradient terms and a trapezoidal implicit treatment of the Coriolis terms will hereinafter be referred to as the SLFBT technique.

The SLFBT technique suffers from the defect that the adjustment terms must still be integrated with a time step which is limited by a CFL condition for gravity-inertia waves. Bates (1983) has developed a method whereby the adjustment terms are integrated by an alternating direction implicit technique while the advective terms are again integrated using the split semi-Lagrangian technique. The new method, referred to as the SLADI method, allows one to take a long time step for adjustment as well as for advection. It has been applied to a one-level version of the modified HIBU model and has been found to give a further gain in efficiency compared to the SLFBT method.

2. ANALYSIS OF SEMI-LAGRANGIAN ADVECTION

We consider the advection equation

$$d\psi/dt = 0 \qquad \text{---(1)}$$

in one and two dimensions. Integrating over the trajectory of a particle which arrives at a grid point P at time $(n+1)\Delta t$ we have

$$\psi^{n+1}(P) = \psi^n_* \qquad \text{---(2)}$$

where ψ^n_* is the value of ψ at the departure point of the particle at time $n\Delta t$. The value of ψ^n_* is obtained by polynomial interpolation from neighboring grid-points, the stability and accuracy of the scheme depending on the type of inter-polation used. We examine five cases of interpolation, all of which reproduce the exact solution at the interpolation gridpoints.

a. One-dimensional flow. Linear interpolation

In this case the situation is as shown in Fig. 1. A constant flow u(we assume $u>0$ without loss of generality) advects a particle from its departure point x_* at time $n\Delta t$ to its arrival gridpoint P at time $(n+1)\Delta t$. The grid interval within which the departure point lies is p grid intervals upstream from the arrival point ($p \geq 0$). We obtain ψ^n_* by linear interpolation from the surrounding gridpoints $(I-p)$ and $(I-p-1)$. Hence (2) gives

$$\psi^{n+1}_I = (1-\hat{\alpha})\psi^n_{I-p} + \hat{\alpha}\psi^n_{I-p-1} \qquad \text{--- (3)}$$

where

$$\hat{\alpha} = \alpha - p \quad , \quad \alpha = u\Delta t/\Delta x$$

Assuming a solution

$$\psi^n_I = \Psi \cdot \lambda^n \exp(ikI\Delta x) \qquad \text{--- (4)}$$

Eq. (3) gives

$$\lambda = \{1 - \hat{\alpha}[1 - \exp(-ik\Delta x)]\}\exp(-ipk\Delta x) \qquad \text{---(5)}$$

If we write

$$\lambda = |\lambda| \exp(-i\omega^*\Delta t)$$

we have

$$|\lambda|^2 = 1 - 2\hat{\alpha}(1-\hat{\alpha})(1-\cos k\Delta x) \qquad \text{---(6)}$$

$$\omega^*\Delta t = pk\Delta x + \tan^{-1}\left[\frac{\hat{\alpha}\sin k\Delta x}{1-\hat{\alpha}(1-\cos k\Delta x)}\right]$$

The scheme is stable $(|\lambda|^2 \leq 1)$, provided

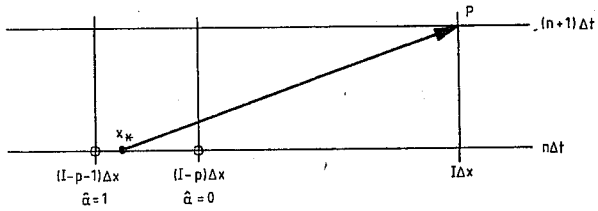

Fig. 1. The two interpolation points used in obtaining ψ_*^n by linear interpolation are circled.

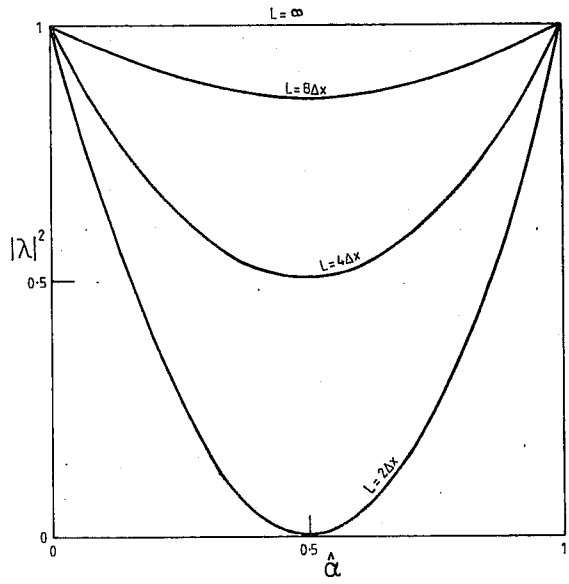

Fig. 2. Squared modulus of the amplification factor as a function of $\hat{\alpha}$ for various wavelengths (case of linear interpolation).

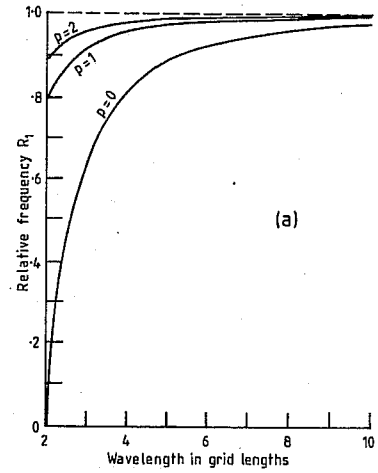

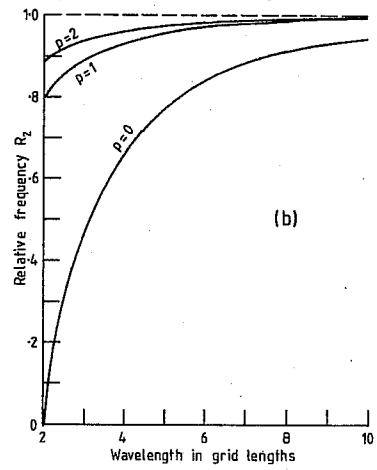

Fig. 3. Relative frequency as a function of wavelength in grid lengths for (a) the case of linear interpolation and (b) the case of quadratic interpolation, for various values of p with $\hat{\alpha} = 0.25$.

$$0 \leq \hat{\alpha} \leq 1 \qquad \text{---(7)}$$

i.e., provided the departure point lies within the interpolation interval $(I - p, I - p - 1)$. But we have chosen the interval so that this is the case; thus the scheme is unconditionally stable.

In Fig. 2, $|\lambda|^2$ is plotted as a function of $\hat{\alpha}$ for various wavelengths L. We see that heavy damping occurs for the shortest wavelengths (complete extinction

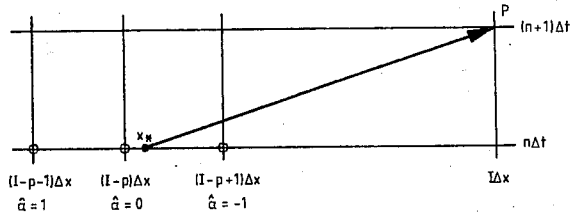

Fig. 4. The three interpolation points used in obtaining ψ_*^n by quadratic interpolation are circled.

of the shortest resolvable wave L = $2\Delta x$ occurs for $\hat{\alpha} = 0.5$), but the damping gets less as the wavelength increases.

Since the analytical frequency ω is given by ku, the relative frequency R_1 $(=\omega^*/\omega)$ is given by

$$R_1 = \frac{1}{(p+\hat{\alpha})k\Delta x} \times \left\{ pk\Delta x + \tan^{-1}\left[\frac{\hat{\alpha}\sin k\Delta x}{1-\hat{\alpha}(1-\cos k\Delta x)} \right] \right\}$$

In the long-wave limit ($k\Delta x \to 0$), we see that $R_1 \to 1$. In Fig. 3(a), R_1 is plotted as a function of wavelength for $\hat{\alpha} = 0.25$. We see that $R_1 \to 1$ as p increases, i.e., the phase errors actually decrease as $u\Delta t/\Delta x$ exceeds unity. This result is, of course, peculiar to the case of a constant wind field, where the departure point can be precisely located using the wind at the arrival point.

b. One-dimensional flow: Quadratic interpolation

In this case the situation is as shown in Fig. 4. The gridpoint nearest the departure point x_* is chosen as the central point of the three interpolation points (I - p + 1), (I - p), (I - p - 1). Thus x_* lies within a half grid interval from (I - p). Using quadratic interpolation, (2) gives

$$\psi_I^{n+1} = 0.5\hat{\alpha}(1+\hat{\alpha})\psi_{I-p-1}^n + (1-\hat{\alpha})(1+\hat{\alpha})\psi_{I-p}^n - 0.5\hat{\alpha}(1-\hat{\alpha})\psi_{I-p+1}^n \qquad ---(8)$$

and assuming a solution of the form (4) we have

$$\lambda = \left[1 - \hat{\alpha}^2(1-\cos k\Delta x) - i\hat{\alpha}\sin k\Delta x \right] \exp(-ipk\Delta x) \qquad ---(9)$$

Thus

$$|\lambda|^2 = 1 - \hat{\alpha}^2(1-\hat{\alpha}^2)(1-\cos k\Delta x)^2 \qquad ---(10)$$

$$\omega^*\Delta t = pk\Delta x + \tan^{-1}\left[\frac{\hat{\alpha}\sin k\Delta x}{1-\hat{\alpha}^2(1-\cos k\Delta x)} \right]$$

The scheme is stable provided

$$-1 \leq \alpha \leq 1 \qquad ---(11)$$

But out interpolation points are chosen such that

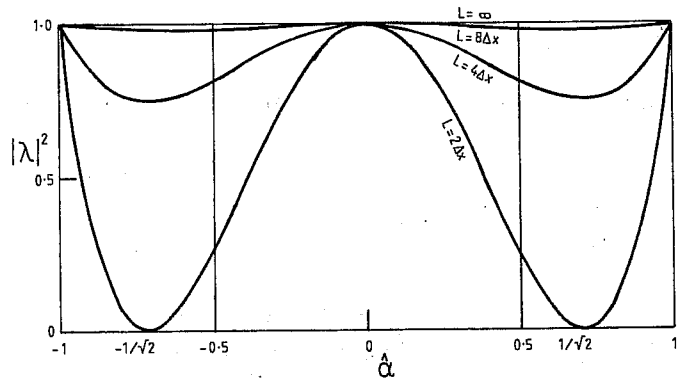

Fig. 5. As in Fig. 2, but for the case of quadratic interpolation.

$$-0.5 \leq \hat{\alpha} \leq 0.5 \qquad \text{---(12)}$$

Thus, this scheme is again unconditionally stable.

In Fig. 5, $|\lambda|^2$ is plotted as a function of $\hat{\alpha}$ for various wavelengths L. Since we choose $\hat{\alpha}$ to lie in the interval defined by (12), we see that complete extinction never occurs and the damping is, in all cases, much less than that given by linear interpolation.

The relative frequency for the case of quadratic interpolation, denoted by R_2, is given by

$$R_2 = \frac{1}{(p+\hat{\alpha})k\Delta x} \times \left\{ pk\Delta x + \tan^{-1}\left[\frac{\hat{\alpha} \sin k\Delta x}{1 - \hat{\alpha}^2(1-\cos k\Delta x)} \right] \right\}$$

Again, in the long-wave limit $R_2 \to 1$, and if the departure point coincides with a gridpoint $R_2 = 1$. In Fig. 3b, R_2 is plotted as a function of wavelength for $\hat{\alpha} = 0.25$. Again we see that $R_2 \to 1$ as p increases. Unlike the amplitude representation, we note that the phase representation is not improved by going to quadratic interpolation.

c. Two-dimensional flow: Bilinear interpolation

In this case the situation is as shown in Fig. 6. The wind components (u,v) are assumed constant and, without loss of generality, positive. Four interpolation points are chosen to surround the departure point (x_*, y_*). The interpolation box is (p,q) grid intervals upstream in the (x,y) directions from the arrival point ($p \geq 0$, $q \geq 0$). Using bilinear interpolation (2) gives

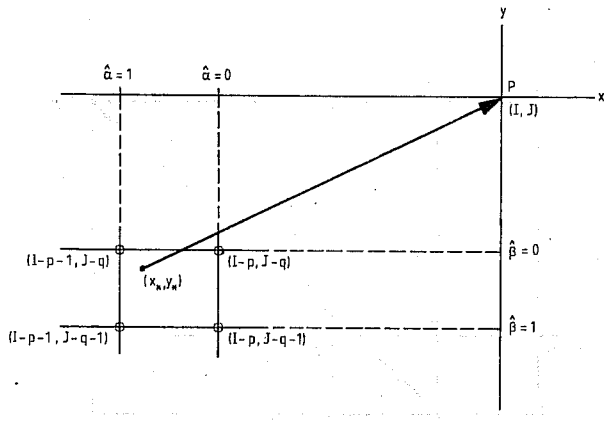

Fig. 6. The four interpolation points used obtaining ψ_*^n by bilinear interpolation are circled.

$$\psi_{I,J}^{n+1} = (1-\hat{\alpha})(1-\hat{\beta})\psi_{I-p,J-q}^{n} + \hat{\alpha}(1-\hat{\beta})\psi_{I-p-1,J-q}^{n}$$
$$+ \hat{\beta}(1-\hat{\alpha})\psi_{I-p,J-q-1}^{n} + \hat{\alpha}\hat{\beta}\psi_{I-p-1,J-q-1}^{n} \qquad \text{---(13)}$$

where $\hat{\alpha}$ is defined as before, and

$$\hat{\beta} = \beta - q \quad , \quad \beta = v\Delta t/\Delta y$$

Assuming a solution

$$\psi_{I,J}^{n} = \Psi^{\circ}\lambda^{n}\exp\left[i(kx+ly)\right] \qquad \text{---(14)}$$

Eq. (13) gives

$$\lambda = \lambda_1\lambda_2$$

where

$$\lambda_1 = \left\{1 - \hat{\alpha}\left[1-\exp(-ik\Delta x)\right]\right\}\exp(-ipk\Delta x) \qquad \text{---(15)}$$

$$\lambda_2 = \left\{1 - \hat{\beta}\left[1-\exp(-il\Delta y)\right]\right\}\exp(-iql\Delta y) \qquad \text{---(16)}$$

i.e., the amplification factor is the product of two factors which are of the same form as in the one-dimensional case of Section 2a. Thus we have the theoretical simplicity of a splitting method, even though no splitting has been used.

A sufficient condition for stability is

$$(0 \leq \hat{\alpha} \leq 1) \quad \text{and} \quad (0 \leq \hat{\beta} \leq 1) \qquad \text{---(17)}$$

which holds if (x_*, y_*) lies within the interpolation box. But this is guaranteed by our initial choice of interpolation points. Thus, the scheme is unconditionally stable.

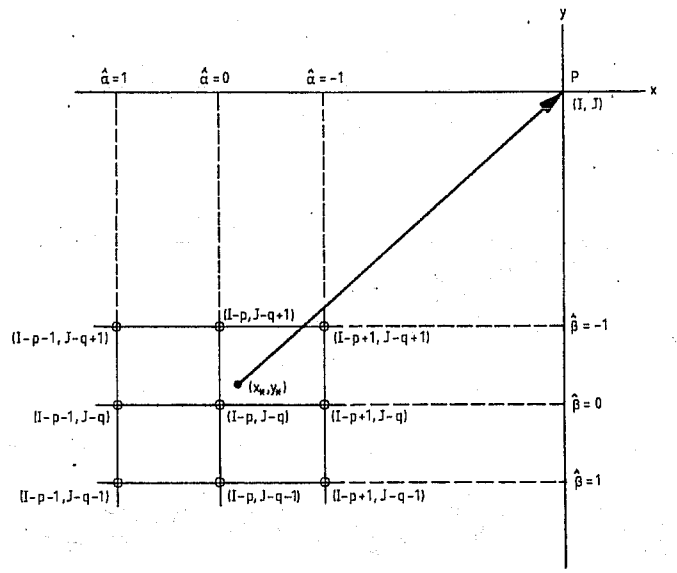

Fig. 7. The nine interpolation points used in obtaining ψ^n_* by biquadratic interpolation are circled

As in the case of Section 2a, heavy damping occurs for the shortest resolvable waves.

d. Two-dimensional flow: Biquadratic interpolation

In this case the situation is as shown in Fig. 7. The grid-point nearest the departure point is chosen as the center of the nine points used in the interpolation. The interpolation formula used is the Lagrangian formula (e.g. Carnahan et al., 1969, p.65).

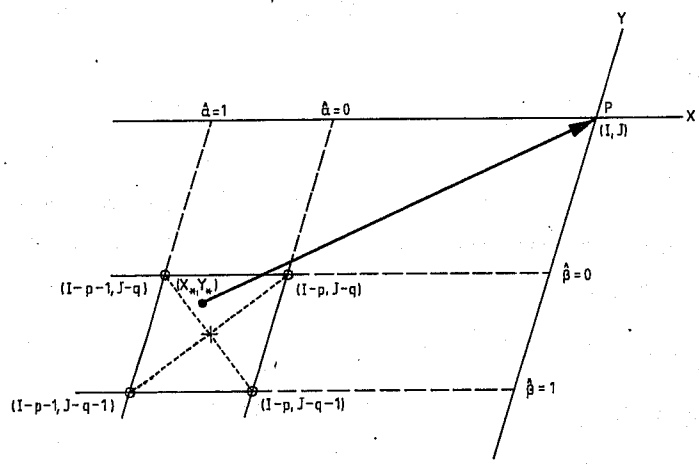

Fig. 8. The four interpolation points used in obtaining ψ^n_* by bilinear interpolation in the oblique axes (X,Y) are circled. The direction of the original orthogonal axes are shown by the dotted lines.

$$\psi^n(x,y) = \sum_{\substack{i=-1 \\ j=-1}}^{\substack{i=1 \\ j=1}} W_{i,j}\, \psi^n_{i,j} \qquad \text{---(18)}$$

where the (i,j) range over the nine interpolation points, and

$$W_{ij} = \prod_{\substack{k=-1 \\ k\neq i}}^{k=1} \frac{(x-x_k)}{(x_i-x_k)} \prod_{\substack{l=-1 \\ l\neq j}}^{l=1} \frac{(y-y_l)}{(y_i-y_l)}$$

This formula reproduces the exact solution at the gridpoints, and when applied to (2) gives

$$\begin{aligned}
\psi^{n+1}_{I,J} = {} & 0.25\hat{\alpha}(1+\hat{\alpha})\hat{\beta}(1+\hat{\beta})\psi^n_{I-p-1,J-q-1} + 0.5(1-\hat{\alpha}^2)\hat{\beta}(1+\hat{\beta})\psi^n_{I-p,J-q-1} \\
& - 0.25\hat{\alpha}(1-\hat{\alpha})\hat{\beta}(1+\hat{\beta})\psi^n_{I-p+1,J-q-1} + 0.5\hat{\alpha}(1+\hat{\alpha})(1-\hat{\beta}^2)\psi^n_{I-p-1,J-q} \\
& + (1-\hat{\alpha}^2)(1-\hat{\beta}^2)\psi^n_{I-p,J-q} - 0.5\hat{\alpha}(1-\hat{\alpha})(1-\hat{\beta}^2)\psi^n_{I-p+1,J-q} \\
& - 0.25\hat{\alpha}(1+\hat{\alpha})\hat{\beta}(1-\hat{\beta})\psi^n_{I-p-1,J-q+1} - 0.5(1-\hat{\alpha}^2)\hat{\beta}(1-\hat{\beta})\psi^n_{I-p,J-q+1} \\
& + 0.25\hat{\alpha}(1-\hat{\alpha})\hat{\beta}(1-\hat{\beta})\psi^n_{I-p+1,J-q+1} \qquad \text{---(19)}
\end{aligned}$$

Assuming a solution of the form (14), we then find

$$\lambda = \lambda_1 \lambda_2$$

where

$$\lambda_1 = \left[1 - \hat{\alpha}^2(1-\cos k\Delta x) - i\hat{\alpha}\sin k\Delta x\right] \exp(-ipk\Delta x)$$

$$\lambda_2 = \left[1 - \hat{\beta}^2(1-\cos l\Delta y) - i\hat{\beta}\sin l\Delta y\right] \exp(-iql\Delta y)$$

i.e., the amplification factor is the product of two factors which are of the same form as in the one-dimensional case (b), so that again we have the theoretical simplicity of a splitting method, without doing any splitting.

A sufficient condition for stability is

$$(-1 \leq \hat{\alpha} \leq 1) \quad \text{and} \quad (-1 \leq \hat{\beta} \leq 1) \qquad \text{--- (20)}$$

But our initial choice of interpolation points is such that

$$(-0.5 \leq \hat{\alpha} \leq 0.5) \quad \text{and} \quad (-0.5 \leq \hat{\beta} \leq 0.5) \qquad \text{--- (21)}$$

Thus the scheme is unconditionally stable.

As in case (b), complete extinction never occurs and the damping is in all cases much less than that given by bilinear interpolation.

e. Two-dimensional flow in an E-grid

The E-grid (see Mesinger and Arakawa, 1976) is a semi-staggered grid in which vector and scalar quantities are expressed at alternate gridpoints. We consider the semi-Lagrangian approach in such a grid for a constant wind field. Bilinear and biquadratic interpolation are most easily defined and analysed if we adopt the axes (X,Y), in general oblique, which run through grid points of a given type (see Fig. 8). Let the wind components in the oblique axes be (u_E, v_E). Then defining

$$\hat{\alpha} = \alpha - p \quad , \quad \alpha = u_E \Delta t / \Delta X$$

$$\hat{\beta} = \beta - q \quad , \quad \beta = v_E \Delta t / \Delta Y$$

we use bilinear interpolation in the (X,Y) coordinates to obtain from (2) an expression of exactly the same form as (13). Assuming a solution

$$\psi^n_{I,J} = \Psi^0 \lambda^n \exp\left[i \left(k_E X + l_E Y \right) \right]$$

we find

$$\lambda = \lambda_1 \lambda_2$$

where

$$\lambda_1 = \left\{ 1 - \hat{\alpha} \left[1 - \exp(-i k_E \Delta X) \right] \right\} \exp(-i p k_E \Delta X)$$

$$\lambda_2 = \left\{ 1 - \hat{\beta} \left[1 - \exp(-i l_E \Delta Y) \right] \right\} \exp(-i q l_E \Delta Y)$$

Thus again a sufficient condition for stability is

$$(0 \leq \hat{\alpha} \leq 1) \quad \text{and} \quad (0 \leq \hat{\beta} \leq 1) \qquad \text{--- (22)}$$

which is guaranteed by our choice of interpolation box.

Similarly, the analysis for the case of biquadratic interpolation in the (X,Y) coordinates proceeds as in (d), giving formally identical results.

3. APPLICATION OF THE SLFBT TECHNIQUE TO A MULTI-LEVEL MODEL

In this section, we describe the results of computations using the SLFBT technique. Operational forecasts made with the HIBU model in its Eulerian form serve as our reference with which to compare the results of the SLFBT integrations.

a. The Eulerian model

The model is a modified version of the HIBU model, developed at the Federal Hydrometeorological Institute and Belgrade University, Yugoslavia (Janjić, 1977, 1979; Mesinger, 1977, 1981). It is a limited area, split explicit, primitive equation model on an E-grid (Arakawa notation), using latitude-longitude coordinates and the sigma vertical coordinate. The model includes a treatment of the divergence term in the continuity equation which prevents the accumulation of two-grid-interval noise. Only very simple physics are employed, moisture and radiation being omitted. There is a simple treatment of surface friction and vertical eddy momentum transport. Dry convective adjustment is applied once every eight time-steps.

The principal modification made to the HIBU model in introducing it into operational use in the Irish Meteorological Service was to rotate the latitude-longitude coordinate system so that the pole was displaced into the Pacific (it now lies at 150^{o}E, 30^{o}N). This gives a much more uniform grid in our area of interest and saves considerably on computer time, since polar filtering is no longer necessary. (The stratagem of rotating a model's spherical coordinate system had previously been used at the Swedish Meteorological and Hydrological Institute; Undén, 1980).

Our integration area, shown in Figs. 9-13, is spanned by 81 X 26 gridpoints carrying the same variable, located at alternate intersections of a 1^{o} X 1^{o} horizontal mesh. Thus the grid distance, defined as the shortest distance between similar points, is 157 km at the model equator. Five levels are used in the vertical, the three upper layers having $\Delta\sigma = 0.25$ and the two lower layers having $\Delta\sigma = 0.125$. The model top is at 200 mb. The time step Δt is 7.5 min, this being imposed by the stability criterion for gravity-inertia waves.

We update the variables on the two outermost boundary lines of the model every time step, using values derived from previous predictions of ECMWF. On the next three lines in from the boundary the integrations are performed using a simple upwind difference scheme for horizontal advection, which gives high damping. In addition, light second-degree diffusive damping is applied on the five outermost boundary lines. Divergence damping (Sadourny, 1975), formulated so as to have no effect on the rotational part of the flow, is applied over the whole area for the full period of the integration, with a coefficient of 1.3×10^{6} $m^{2}s^{-1}$.

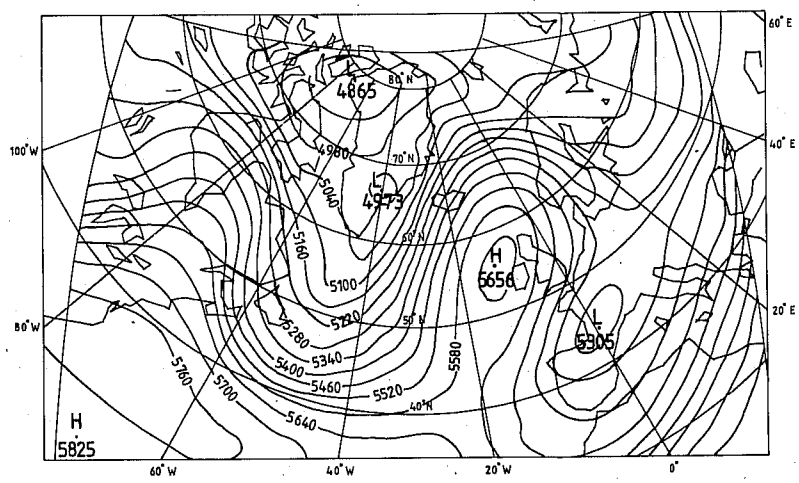

Fig. 9. 24 h 500 mb forecast for 31 March 1982 at 0000 GMT, performed with the Eulerian model. Time step 7.5 min for all terms. Contours in gpm.

The model as described above was used operationally between July 1980 and May 1982 to produce 36 h forecasts twice a day on a DEC 20/50 computer having a speed of approximately 1 MIPS and a core storage of 256 K words. The model resides in core. Using an Adams-Bashforth time scheme for the horizontal advection terms, which was found most satisfactory in operational practice, the CPU time required for a 24 h integration was 37 min, of which 17 min was spent on the horizontal advection.

b. Attempts to use multiple time steps for advection in the Eulerian model

In a model based on the splitting method, the separate phases of the integration have their own stability criteria. In principle, therefore, it is possible to economize on computer time by using a multiple time step for the advective terms, since these have a more lenient stability criterion than do the adjustment terms.

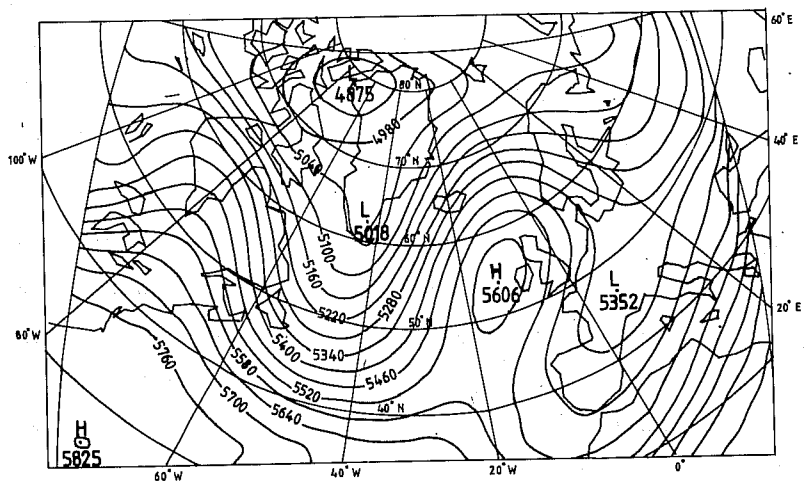

Fig. 10. As in Fig. 9, but performed with the model having semi-Lagrangian advection. Case of bilinear interpolation. Adjustment time step 7.5 min, advection time step 30 min.

We have made numerous attempts to use this theoretical advantage of the splitting method in the framework of our Eulerian model, but without success.

With the single step Adams-Bashforth or Euler-forward time schemes for horizontal advection, we have found it possible to ensure stability only by using the same time step Δt for advection as is used for adjustment. With the two step Heun scheme, we have been able to achieve a time step of $2\Delta t$ for advection. However, there is no net saving of computer time in this case, since the additional intermediate calculations required by the Heun scheme cancel the advantage of using a double time step.

As far as we are aware, no other users of split explicit Eulerian models have been able to use multiple time steps for advection with a single step time scheme. Marchuk (1974), in his textbook devoted mainly to the splitting method, does not refer to any such application. Janjić (personal communication, 1980) and others (Gadd, 1978; Duffy, 1981) have succeeded in using $3\Delta t$ for advection, but in all cases in combination with a two-step time scheme requiring intermediate calculations.

c. The model with semi-Lagrangian advection

We now modify the Eulerian model by taking the horizontal advection terms in the momentum and thermodynamic equations and expressing them in the form $(du/dt)_H = 0$, $(dv/dt)_H = 0$, $(dT/dt)_H = 0$. We integrate these terms in the semi-Lagrangian manner, chosing a multiple time step $N\Delta t$. The remaining terms are kept in their original Eulerian form and integrated as before with the single time step Δt.

On arriving at a time $n\Delta t$ in the cycle of integration when a horizontal advection step is to be performed, the departure points of particles which will arrive at the gridpoints (I,J) at time $(n + N)\Delta t$ are first estimated. This is done by taking the available wind components $(u,v)^n_{I,J}$, regarding them as valid at $(n + N/2)\Delta t$, and using them to go back from the gridpoints over the interval $N\Delta t$ to find the departure points at time $n\Delta t$. (A time truncation error enters here, of course; it can be reduced by adopting an iterative procedure - see below.) Gridpoints surrounding the departure points are chosen as interpolation points, in the manner described in Secion 2. The advective integration is then performed according to the formula

$$\psi^{n+N}_{I,J} = \psi^n_* \qquad \text{---(23)}$$

where ψ^n_* is evaluated by bilinear or biquadratic interpolation in the (X,Y) coordinates of the E-grid, as described in Subsection 2e.

The above description refers to the integration of the momentum equations. In the case of the thermodynamic equation, where wind components are not available at the relevant gridpoints, the trajectories are estimated using winds obtained by four-point spatial averaging.

The advective step is followed by N applications of the adjustment step, acting in the first instance on the values $\psi_{I,J}^{n+N}$ obtained from (23).

Numerical experiments have been performed with the model thus modified, for the cases of both bilinear and biquadratic interpolation. All non-advective parameters have been kept at the same values as in the Eulerian model. With the semi-Lagrangian approach we have found it possible, for the first time, to use multiple time steps for advection without having to employ an intermediate time stepping procedure within this phase.

The integrations for the bilinear case, though very efficient and completely stable, have been found to give undesirably smooth forecast charts; this is in accord with the analysis of Section 2. We show in Fig. 9 a 24 h 500 mb forecast performed with our Eulerian model. The corresponding bilinear semi-Lagrangian forecast with an advective time step of $4\Delta t$ is shown in Fig. 10. Though the patterns are similar, it can be seen that considerable smoothing has taken place. The CPU time spent on the horizontal advection phase, however, has been reduced from 17 to 3 min for the 24 h integration, representing an overall saving of 38% (the time taken from the adjustment phase remains unchanged).

The results for the case of biquadratic interpolation are much more satisfactory. We show in Fig. 11 the corresponding forecast for this case, again using $4\Delta t$ for advection. Comparing this with the Eulerian forecast we see that the results are very close. The time now taken for the advective phase is 4 min for the 24 h integration, representing an overall saving in CPU time of 35% compared to the Eulerian run.

In this biquadratic semi-Lagrangian run, the advective time step was large enough so that 201 vector points and 188 scalar points (mostly at the top level) had p or q greater than zero at the beginning of the integration. After 24 h, 157 vector points and 145 scalar points still had p or q greater than zero. Thus, the multiply-upstream interpolation was being fully used.

Sixty 36 h forecasts were run in parallel over the period 6 April-8May 1982 to compare the bi-quadratic semi-Lagrangian model as described above with the Eulerian model. In all cases, the integrations remained stable, and subjective comparison showed no significant differences between the two sets of forecasts. Some objective verification statistics derived from these runs are shown in Table 1.

TABLE 1. Verification statistics for the Eulerian model, and the biquadratic semi-Lagrangian model with a time step of $4\Delta t$ for advection, for sixty 24 h (36 h) forecasts. The statistics were evaluated on a central verification area.

	Eulerian model	Biquadratic semi-Lagrangian model
rms error (m) in 500 mb geopotential	34.37 (48.90)	32.78 (46.90)
Standard error in the mean (m) in 500 mb geopotential	1.29 (1.94)	1.18 (1.82)
rms error (mb) in surface pressure	3.72 (5.12)	3.70 (5.15)
Standard error in the mean (mb) in surface pressure	0.15 (0.20)	0.15 (0.19)

No loss of accuracy is indicated on going over to the semi-Lagrangian model, despite its longer advective time step.

As a result of these tests, the biquadratic semi-Lagrangian model with the time step of $4\Delta t$ for advection has been adopted for operational use in the IMS, beginning on 10 May 1982. In addition to economy in computer time, the semi-Lagrangian model has the advantage of requiring less computer storage than the Eulerian model. This is due to the fact that the Eulerian model with the Adams-Bashforth time scheme for advection required storage of the three-dimensional arrays relating to the advection of (u, v, T) at the previous as well as the current time level.

To further test the properties of the biquadratic semi-Lagrangian model, we have

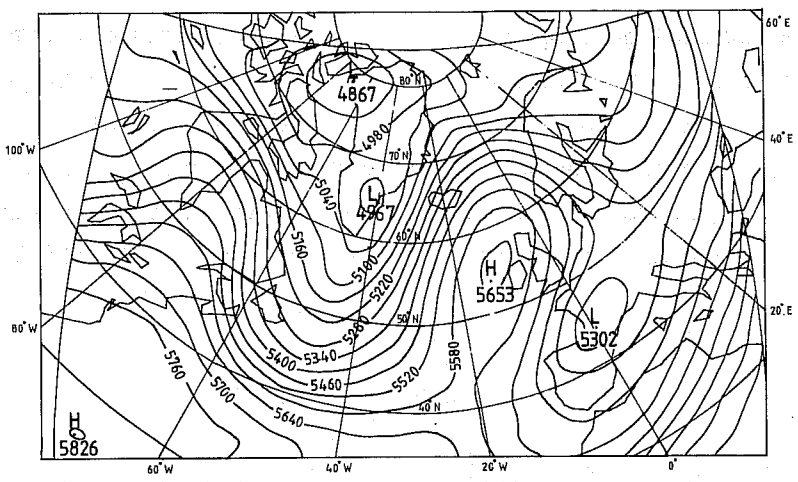

Fig. 11. As in Fig. 10, but for case of bi-quadratic interpolation.

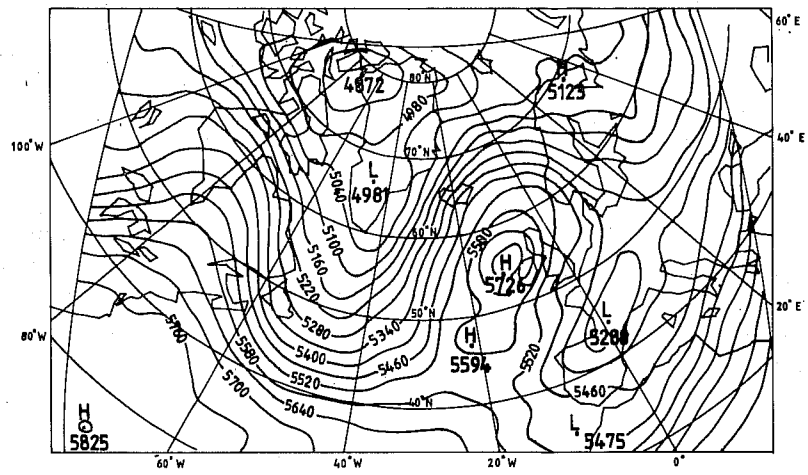

Fig. 12. As in Fig. 11, but with an advection time step of 1 h.

performed a number of 36 h integrations using an advective time step of $8\Delta t$. The integrations have all remained stable, though localized noise is evident on some of the forecast charts. As an example, the 24 h forecast corresponding to Fig. 9 is shown in Fig. 12. In addition to the appearance of noise, there has been a noticeable loss of accuracy compared to the Eulerian forecast. In the present case, 1949 vector points and 1954 scalar points had p or q greater than zero at the beginning of the integration, while the corresponding figures after 24 h are 1749 and 1725, respectively. Extensive use was therefore being made of the multiply-upstream interpolation. Our subjective impression is that the noise arises in regions where significant changes in wind speed or direction occur.

In an effort to reduce the noise and increase the accuracy of the integration having an $8\Delta t$ advective time step, we have performed some experiments in which the departure points are estimated using an iterative procedure. As a first step in

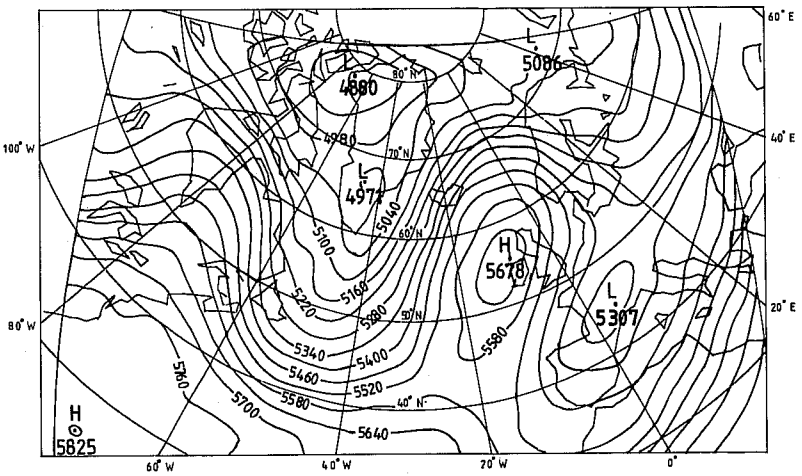

Fig. 13. As in Fig. 12, but with position of departure points estimated using an interative procedure.

the iteration, we proceed as before, using $(u, v)^{n}_{I,J}$ to estimate the departure points of particles which arrive at the grid-points (I,J) at time $(n + 8)\Delta t$. A first biquadratic semi-Lagrangian update is performed and the values $(u,v)^{n+8}_{I,J}$ obtained are regarded as provisional. An average of the velocity components $(u,v)^{n}_{I,J}$ and $(u,v)^{n+8}_{I,J}$ is then taken, and the departure points are re-estimated using these average values. This is followed by a second biquadratic semi-Lagrangian update, again acting on the time level n quantities, giving the new values $(u, v, T)^{n+8}_{I,J}$. The results of a 24 h integration using this iterative procedure, valid for the same time as Fig. 9, are shown in Fig. 13. The forecast is indeed more accurate (relative to the Eulerian forecast) and less nosiy than Fig. 12, but not as accurate or as noisefree as Fig. 11, where a $4\Delta t$ advective time step was used without iteration. The CPU time required by the iterative run was almost the same as that required for the forecast of Fig. 11. For a given expenditure of computer time, therefore, it appears preferable to use shorter time steps without iteration, rather than longer time steps with iteration.

Finally we note that Robert (1981) has used bicubic interpolation in his integrations, which he finds to be expensive. Our results would seem to indicate that the biquadratic is as high an order of interpolation as is required.

4. THE SLADI SCHEME

An alternating direction implicit method was developed by Leendertse (1967) for integrating the shallow water equations in the hydraulic engineering context. From the meteorological viewpoint, Leendertse's scheme suffers from the defects that the advective terms are computationally unstable and that there is no simple numerical solution corresponding to a Rossby wave. In the SLADI scheme presented by Bates (1983), these defects have been eliminated. The scheme is based on the following splitting of the shallow water equations:-

$$\begin{cases} \dfrac{du}{dt} = 0 & \text{---(23)} \\ \dfrac{dv}{dt} = 0 & \text{---(24)} \\ \dfrac{d\phi}{dt} = 0 & \text{---(25)} \end{cases} \qquad \begin{cases} \dfrac{\partial u}{\partial t} = -\dfrac{1}{a\cos\theta}\dfrac{\partial \phi}{\partial \lambda} + \left(f + \dfrac{u\tan\theta}{a}\right)v & \text{---(26)} \\ \dfrac{\partial v}{\partial t} = -\dfrac{1}{a}\dfrac{\partial \phi}{\partial \theta} - \left(f + \dfrac{u\tan\theta}{a}\right)u & \text{---(27)} \\ \dfrac{\partial \phi}{\partial t} = -\left[\bar{\phi} + \phi'\right]\left[\dfrac{1}{a\cos\theta}\dfrac{\partial u}{\partial \lambda} + \dfrac{1}{a\cos\theta}\dfrac{\partial}{\partial \theta}\left(v\cos\theta\right)\right] & \text{---(28)} \end{cases}$$

Where $\bar{\phi}$ is the mean geopotential and ϕ' is the deviation therefrom.

The advective equations (23)-(25) are integrated using the multiply-upstream semi-Lagrangian scheme with biquadratic interpolation, as described in Bates and McDonald (1982). The advective time step is Δt_{adv}.

The adjustment equations (26)-(28) are integrated in two steps. In the first, λ -derivatives (in linear terms) are treated implicitly while θ -derivatives are treated explicitly; in the second, Θ -derivatives (in linear terms) are treated implicitly while λ -derivatives are treated explicitly. All non-linear terms are treated in an effectively explicit manner. The adjustment time step is Δt_{adj}. Thus we have:

Step 1.

$$\frac{v^{n+1/2}_{I,J} - v^{n}_{I,J}}{\tau} = -\frac{1}{a}\left[\frac{\phi^{n}_{I,J+1} - \phi^{n}_{I,J-1}}{2\Delta\theta}\right] - \mathcal{F}^{n}_{I,J}\, u^{n}_{I,J} \qquad \cdots (29)$$

$$\left[\begin{aligned}
&\frac{u^{n+1/2}_{I,J} - u^{n}_{I,J}}{\tau} = -\frac{1}{a\cos\theta(J)}\left[\frac{\phi^{n+1/2}_{I+1,J} - \phi^{n+1/2}_{I-1,J}}{2\Delta\lambda}\right] + \mathcal{F}^{n}_{I,J}\, v^{n+1/2}_{I,J} && \cdots (30)\\
&\frac{\phi^{n+1/2}_{I',J} - \phi^{n}_{I',J}}{\tau} = -\frac{1}{a\cos\theta(J)}\left[\overline{\phi}\left(\frac{u^{n+1/2}_{I'+1,J} - u^{n+1/2}_{I'-1,J}}{2\Delta\lambda}\right) + (\phi')^{n}_{I',J}\left(\frac{u^{n}_{I'+1,J} - u^{n}_{I'-1,J}}{2\Delta\lambda}\right)\right]\\
&\qquad\qquad - \frac{\phi^{n}_{I',J}}{a\cos\theta(J)}\left[\frac{(\hat{v})^{n}_{I',J+1} - (\hat{v})^{n}_{I',J-1}}{2\Delta\theta}\right] && \cdots (31)
\end{aligned}\right.$$

Step 2.

$$\frac{u^{n+1}_{I,J} - u^{n+1/2}_{I,J}}{\tau} = -\frac{1}{a\cos\theta(J)}\left[\frac{\phi^{n+1/2}_{I+1,J} - \phi^{n+1/2}_{I-1,J}}{2\Delta\lambda}\right] + \mathcal{F}^{n+1/2}_{I,J}\, v^{n+1/2}_{I,J} \qquad \cdots (32)$$

$$\left[\begin{aligned}
&\frac{v^{n+1}_{I,J} - v^{n+1/2}_{I,J}}{\tau} = -\frac{1}{a}\left[\frac{\phi^{n+1}_{I,J+1} - \phi^{n+1}_{I,J-1}}{2\Delta\theta}\right] - \mathcal{F}^{n+1/2}_{I,J}\, u^{n+1}_{I,J} && \cdots (33)\\
&\frac{\phi^{n+1}_{I,J'} - \phi^{n+1/2}_{I,J'}}{\tau} = -\frac{1}{a\cos\theta(J')}\left[\overline{\phi}\left(\frac{(\hat{v})^{n+1}_{I,J'+1} - (\hat{v})^{n+1}_{I,J'-1}}{2\Delta\theta}\right) + (\phi')^{n+1/2}_{I,J'}\left(\frac{(\hat{v})^{n+1/2}_{I,J'+1} - (\hat{v})^{n+1/2}_{I,J'-1}}{2\Delta\theta}\right)\right]\\
&\qquad\qquad - \frac{\phi^{n+1/2}_{I,J'}}{a\cos\theta(J')}\left[\frac{u^{n+1/2}_{I+1,J'} - u^{n+1/2}_{I-1,J'}}{2\Delta\lambda}\right] && \cdots (34)
\end{aligned}\right.$$

where

$$\tau = \Delta t_{adj}/2 \quad , \quad (\hat{v})^{n}_{I,J} = (v\cos\theta)^{n}_{I,J} \quad , \quad \mathcal{F}^{n}_{I,J} = \left(f + \frac{u\tan\theta}{a}\right)^{n}_{I,J}$$

The indices (I,J) denote vector points in our semi-staggered E grid, while (I,J') and (I',J) denote scalar points.

In Step 1 the v-equation, being explicit, is integrated first and the u and ϕ equations are then integrated together as a coupled implicit pair (see below), while in Step 2 the u-equation is integrated first and the v and ϕ-equations are then integrated as a coupled pair.

In all the SLADI numerical experiments described later, we alternate the order in which Steps 1 and 2 are performed. This increases the symmetry of the scheme and gives results slightly closer to the reference SLFBT integration than when the order is not alternated.

The integration domain is identical to that used for the SLFBT experiments described earlier. Apart from the replacement of the SLFBT by the SLADI method of integration, the only other difference is that in the present case the boundary conditions are held fixed.

Method of solving the implicit equations

The first pair of implicit equations (30) and (31) can be written

$$\alpha_1(J)\,\phi^{n+1/2}_{I+1,J} + u^{n+1/2}_{I,J} - \alpha_1(J)\,\phi^{n+1/2}_{I-1,J} = E(I,J) \qquad \text{---(35)}$$

$$\bar{\phi}\,\alpha_1(J)\,u^{n+1/2}_{I'+1,J} + \phi^{n+1/2}_{I',J} - \bar{\phi}\,\alpha_1(J)\,u^{n+1/2}_{I'-1,J} = E(I',J) \qquad \text{---(36)}$$

where

$$\alpha_1(J) = \tau / 2a\cos\theta(J)\,\Delta\lambda \quad , \quad \alpha_2(J) = \tau / 2a\cos\theta(J)\,\Delta\theta$$

$$E(I,J) = u^{n}_{I,J} + \tau\, f^{n}_{I,J}\, v^{n+1/2}_{I,J} \qquad \text{---(37)}$$

$$E(I',J) = \phi^{n}_{I',J}\left[1 - \alpha_2(J)\left(\hat{v}^{n}_{I',J+1} - \hat{v}^{n}_{I',J-1}\right)\right] - \left(\phi'\right)^{n}_{I',J}\,\alpha_1(J)\left(u^{n}_{I'+1,J} - u^{n}_{I'-1,J}\right) \qquad \text{---(38)}$$

In (35) and (36) all quantities at the new time level appear on the l.h.s. while all non-linear terms occur on the r.h.s.

Supposing first that we are on a line with an even value of J, where the end points are vector points, we can write the pair of equations (35), (36) in the form

$$A_I W_{I+1} + W_I - A_I W_{I-1} = E_I \;;\; 3 \le I \le (I_M - 2) \qquad \text{---(39)}$$

where I has a range $(1, I_M)$ and

$$A_I = \begin{cases} \bar{\phi}\,\alpha_1(J), & I \text{ even} \\ \alpha_1(J), & I \text{ odd} \end{cases} \qquad \text{---(40)}$$

$$\left[W_2, W_3, \cdots W_{I_M-1}\right] = \left[\left(\phi^{n+1/2}_{2,J}\right), \left(u^{n+1/2}_{3,J}\right), \cdots\cdots, \left(\phi^{n+1/2}_{I_M-1,J}\right)\right] \qquad \text{---(41)}$$

$$\left[E_3, E_4, \cdots E_{I_M-2}\right] = \left[E(3,J), E(4,J), \cdots\cdots, E(I_M-2,J)\right] \qquad \text{---(42)}$$

For convenience, the J-subscripts have been suppressed in the quantities (A_I, W_I, E_I). We solve (39) by assuming a recursion formula

$$W_I = -P_I W_{I+1} + Q_I \quad ; \quad 2 \leq I \leq I_M - 2 \qquad \text{---(43)}$$

from which it follows that

$$W_{I-1} = -P_{I-1} W_I + Q_{I-1}$$

Using this to eliminate W_{I-1} from (39) gives

$$W_I = -\left[\frac{A_I}{1 + A_I P_{I-1}}\right] W_{I+1} + \left[\frac{A_I Q_{I-1} + E_I}{1 + A_I P_{I-1}}\right]$$

whence we have, by comparison with (43),

$$P_I = \frac{A_I}{1 + A_I P_{I-1}} \quad , \quad Q_I = \frac{A_I Q_{I-1} + E_I}{1 + A_I P_{I-1}} \quad ; \quad 3 \leq I \leq I_M - 2 \qquad \text{---(44)}$$

As boundary conditions on the solution of (39) we require

$$W_2 \equiv \phi^{n+1/2}_{2,J} = \phi^n_{2,J} \qquad \text{---(45)}$$

$$W_{I_M-1} \equiv \phi^{n+1/2}_{I_M-1,J} = \phi^n_{I_M-1,J} \qquad \text{---(46)}$$

In order that (43) hold at $I = 2$ we require, using (45),

$$\phi^n_{2,J} = -P_2 u^{n+1/2}_{3,J} + Q_2$$

In order that this hold for arbitrary $u^{n+1/2}_{3,J}$ we must have

$$P_2 = 0, \quad Q_2 = \phi^n_{2,J} \qquad \text{---(47)}$$

Starting with the values given by (47), we sweep from left to right using (44) to calculate the (P_I, Q_I) for all doubly-interior points. Then starting with W_{I_M-1} as given by (46), we sweep from right to left using (43) to calculate the W_I for all doubly-interior points. Thus, all the $(n + \frac{1}{2})$-level quantities for even values of J are determined.

Supposing next that we are on a line with an odd value of J, where the end points are scalar points, we can write the pair of equations (35), (36) again in the form (39) provided we now define

$$A_I = \begin{cases} \alpha_1(J), & I \text{ even} \\ \bar{\phi}\,\alpha_1(J), & I \text{ odd} \end{cases} \qquad \text{---(48)}$$

$$\left[W_2, W_3, \cdots, W_{I_M-1}\right] = \left[\left(u_{2,J}^{n+1/2}\right), \left(\phi_{3,J}^{n+1/2}\right), \cdots, \left(u_{I_M-1,J}^{n+1/2}\right)\right]$$

The solution proceeds as before, the boundary conditions corresponding to (45), (46) now being

$$W_2 \equiv u_{2,J}^{n+1/2} = u_{2,J}^{n} \qquad \text{---(49)}$$

$$W_{I_M-1} \equiv u_{I_M-1,J}^{n+1/2} = u_{I_M-1,J}^{n} \qquad \text{---(50)}$$

The starting values (P_2, Q_2) corresponding to (47) are now given by

$$P_2 = 0, \quad Q_2 = u_{2,J}^{n} \qquad \text{---(51)}$$

The remaining (P_I, Q_I) are again determined by a left-to-right sweep and the W_I by a right-to-left sweep, using the same formulae as before.

The second pair of implicit equations (33), (34) can be written

$$\alpha_3(J)\,\phi_{I,J+1}^{n+1} + \hat{v}_{I,J}^{n+1} - \alpha_3(J)\,\phi_{I,J-1}^{n+1} = \hat{E}(I,J) \qquad \text{---(52)}$$

$$\bar{\phi}\,\alpha_2(J')\,\hat{v}_{I,J'+1}^{n+1} + \phi_{I,J'}^{n+1} - \bar{\phi}\,\alpha_2(J')\,\hat{v}_{I,J'-1}^{n+1} = \hat{E}(I,J') \qquad \text{---(53)}$$

where

$$\alpha_3(J) = \tau \cos\theta(J) / 2a\Delta\theta$$

$$\hat{E}(I,J) = \cos\theta(J)\left[v_{I,J}^{n+1/2} - \tau f_{I,J}^{n+1/2} u_{I,J}^{n+1}\right] \qquad \text{---(54)}$$

$$\hat{E}(I,J') = \phi_{I,J'}^{n+1/2}\left[1 - \alpha_1(J')\left(u_{I+1,J'}^{n+1/2} - u_{I-1,J'}^{n+1/2}\right)\right]$$
$$- \left(\phi'\right)_{I,J'}^{n+1/2} \alpha_2(J')\left(\hat{v}_{I,J'+1}^{n+1/2} - \hat{v}_{I,J'-1}^{n+1/2}\right) \qquad \text{--- (55)}$$

This pair of coupled equations are solved by a method exactly analogous to that described above, where the direction of sweep is now up and down.

We note that the P_I and the denominators of the Q_I, as defined by (44), do not depend on the time step and therefore need to be computed once only, thereby increasing the efficiency of the integration.

Stability of the above method of solving the tridiagonal system (39) requires

diagonal dominance (Isaacson and Keller, 1966, p.56). To show that this indeed obtains, we use (36) to eliminate the $\phi^{n+1/2}$ from (35), giving

$$\bar{\phi}\left[\alpha_1(J)\right]^2 u^{n+1/2}_{I+2,J} - \left\{1 + 2\bar{\phi}\left[\alpha_1(J)\right]^2\right\} u^{n+1/2}_{I,J} + \bar{\phi}\left[\alpha_1(J)\right]^2 u^{n+1/2}_{I-2,J}$$

$$= \alpha_1(J)\left[E(I+1,J) - E(I-1,J)\right] - E(I,J)$$

Clearly the absolute value of the coefficient of the diagonal term exceeds the sum of the coefficients of the off-diagonal terms, so that numerical stability of the method is assured, regardless of the time step. The same considerations apply to the pair (52), (53).

5. APPLICATION OF THE SLADI SCHEME TO A ONE-LEVEL MODEL

The theoretical properties of the SLADI scheme are analysed in Bates (1983). Here we present some results of 24-hour numerical integrations using the SLADI scheme as applied to a one-level model representing the 500 mb level. The integrations start from the analysis for 00Z on 21 May 1982 as shown in Fig. 14. In all cases, $\bar{\phi}$ corresponds to the standard atmosphere value for the 500 mb level.

As a reference, we show in Fig. 15 the one-level 24-hour forecast using the SLFBT scheme with Δt_{adv} = 30 min, Δt_{adj} = 7.5 min. As the SLADI integrations to be described below do not include any mechanism for suppressing two-grid interval noise, we omit the noise suppressor in the reference integration also. The CPU time taken for the reference integration is then 138.5 sec.

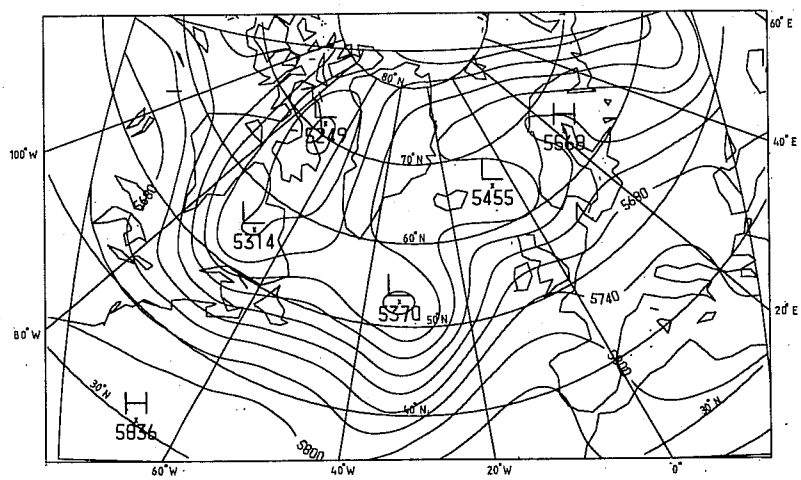

Fig. 14 500 mb analysis for 00Z on 21 May 1982

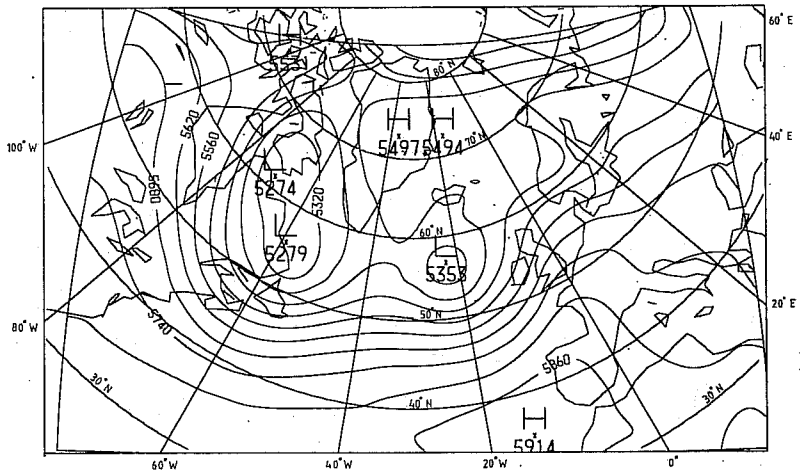

Fig. 15 24 hr 500 mb reference integration using the SLFBT scheme with Δt_{adv} = 30 min, Δt_{adj} = 7.5 min (Biquadratic interpolation)

The results of a 24-hour integration using the SLADI scheme with Δt_{adv} = 30 min, Δt_{adj} = 7.5 min are shown in Fig. 16. The cycle of integration is (A-1-2-2-1-1-2-2-1), where A refers to an advective step and (1,2) refer to step 1 and 2 of the adjustment scheme. It can be seen that the results are very similar to those of the reference integration. The maximum height differences which occur are of 15m in the neighbourhood of the low centres, representing a slight smoothing by comparison with the reference run. The differences away from the low centres are negligible. The CPU time taken for the integration is 210.3 sec, representing an increase of 52% over the reference run.

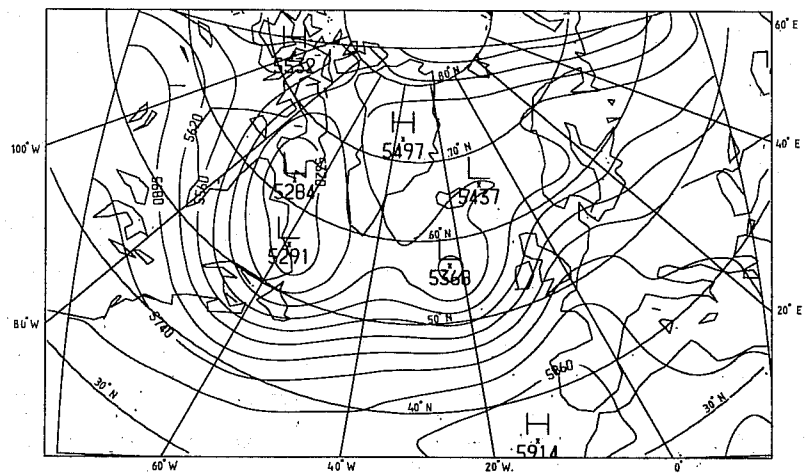

Fig. 16 24 hr 500 mb integration using the SLADI scheme with Δt_{adv} = 30 min, Δt_{adj} = 7.5 min (Biquadratic interpolation)

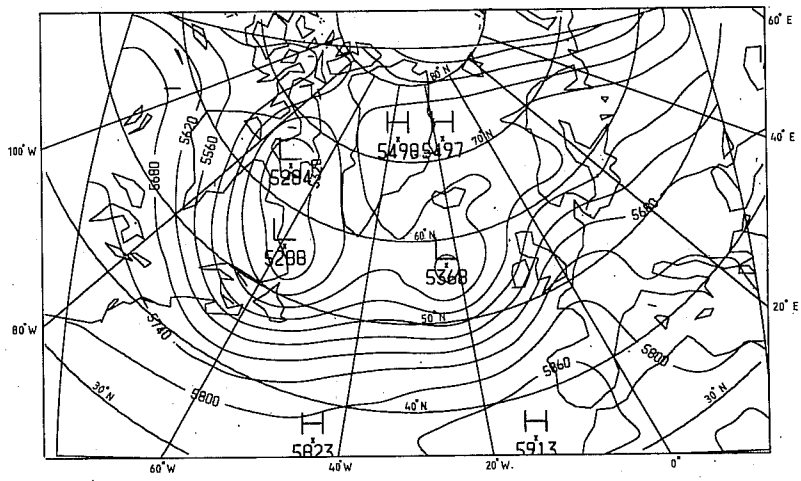

Fig. 17 24 hr 500 mb integration using the SLADI scheme with $\Delta t_{adv} = \Delta t_{adj}$ = 30 min (Biquadratic interpolation)

We now quadruple the adjustment time step while holding the advection time step unchanged and integrate with the cycle (A-1-2-A-2-1). The integration remains stable, the results being shown in Fig. 17. The differences between Figs. 16 and 17 are less than 5m over nearly all of the chart and at only one point amount to 10 m. Quadrupling the adjustment time step does not appear to have led to any disimprovement of the forecast by comparison with the reference run. The CPU time is now 81.6 sec, representing a saving of 41% over the reference run.

As regards the smoothing of both SLADI integrations by comparison with the reference run, we note that an SLFBT integration with $\Delta t_{adv} = \Delta t_{adj}$ = 100 sec gives even greater smoothing, the low centres being up to 20m less deep than those of Fig. 15. Thus, it is difficult to say which of the integrations described above is most accurate. This question can best be decided by using both schemes in a multi-level model, running a large number of forecasts and comparing the results with what happens in the real atmosphere.

6. CONCLUSIONS

The split semi-Lagrangian method of integrating the advective terms has been combined with two methods of integrating the adjustment terms in primitive equation models.

In the first, the SLFBT method, the adjustment terms are integrated using a forward-backward technique for the gravity wave terms and a trapezoidal implicit method for the Coriolis terms. This allows a long time step for advection but still requires a short time step for adjustment, as determined by the CFL condition for gravity waves. The method has been applied to a multilevel PE model with variable boundary

conditions and shown to lead to a saving of a third of the CPU time required to integrate the model in Eulerian form.

In the second, the SLADI method, the adjustment terms are integrated using an alternating direction implicit scheme, where all non-linear components of the adjustment terms are treated in an explicit manner. The adjustment integration is then carried out in two steps, where each involves only the solution of a simple tri-diagonal system. The method allows one to take equally long time steps for adjustment as for advection. When applied to a one-level PE model with fixed boundary conditions, it leads to a further saving of CPU time amounting to 40% by comparison with the SLFBT method, while giving comparable accuracy.

REFERENCES

Bates, J.R., 1983: An efficient semi-Lagrangian and alternating direction implicit method for integrating the shallow water equations. (manuscript in preparation).

Bates, J.R. and A. McDonald, 1982: Multiply-upstream, semi-Lagrangian advective schemes: analysis and application to a multi-level primitive equation model. Mon. Wea. Rev., 110, 1831 - 1842.

Carnahan, B., H.A. Luther and J.O. Wilkes, 1969: Applied Numerical Methods, Wiley, 604 pp.

Duffy, D.G., 1981: A split explicit reformulation of the regional numerical weather prediction model of the Japan Meteorological Agency. Mon. Wea. Rev., 109, 931-945.

Gadd, A.J., 1978: A split explicit integration scheme for numerical weather prediction. Quart. J. Roy. Meteor. Soc., 104, 569-582.

Isaacson, E. and H.B. Keller, 1966: Analysis of Numerical Methods, Wiley, 541 pp.

Janjić, Z., 1977: Pressure gradient force and advection scheme used for forecasting with steep and small scale topography. Contrib. Atmos. Phys., 50, 186-199.

_____, 1979: Forward-backward scheme modified to prevent two-grid intervel noise and its application in the σ-coordinate models. Contrib. Atmos. Phys., 52, 69-84.

Leendertse, J., 1967: Aspects of a computational model for long-period water-wave propagation. Rand Memorandum RM-5294-PR. The Rand Corporation, Santa Monica, California.

Marchuk, G.I., 1974: Numerical Methods in Weather Prediction. Academic Press, 277 pp. (Russian ed., 1967)

McDonald, A., 1983: Accuracy of multiply-upstream, semi-Lagrangian advective schemes. (Submitted to Mon. Wea. Rev.)

Mesinger, F., 1977: Forward-backward scheme and its use in a limited area model. Contrib. Atmos. Phys., 50, 200-210.

_____, 1981: Horizontal advection schemes of a staggered grid; an energy

and enstrophy conserving model. Mon. Wea. Rev., 109, 467-478.

———— and A. Arakawa, 1976: Numerical methods used in atmospheric models. Vol. 1, GARP Publ. Ser., No. 17, WMO-ICSU, 64 pp.

Robert, A., 1981: A stable numerical integration scheme for the primitive meteorological equations. Atmos. Ocean, 19, 35-46.

————, 1982: A semi-Lagrangian and semi-implicit numerical integration scheme for the primitive meteorological equations. J. Met. Soc. Japan, 60, 319-324

Sadourny, R., 1975: The dynamics of finite-difference models of the shallow-water equations. J. Atmos. Sci., 32, 680-689.

Undén, P., 1980: Changing the spherical grid for LAMS. Limited area Modelling Newsletter 1, No. 1, pp. 12-16. (Available from SMHI, Box 923, Norrköping, Sweden).